Chen et al. *Boundary Value Problems* (2019) 2019:34
https://doi.org/10.1186/s13661-019-1151-y

Boundary Value Problems
a SpringerOpen Journal

RESEARCH **Open Access**

Method of fundamental solutions for a Cauchy problem of the Laplace equation in a half-plane

Bo Chen[1], Yao Sun[1*] and Zibo Zhuang[2]

*Correspondence:
syhf2008@gmail.com
[1] College of Science, Civil Aviation University of China, Tianjin, China
Full list of author information is available at the end of the article

Abstract

This paper is to provide an analysis of an ill-posed Cauchy problem in a half-plane. This problem is novel since the Cauchy data on the accessible boundary is given, whilst the additional temperature is involved on a line. The *Dirichlet boundary condition on part of the boundary is an essential condition* in the physical meaning. Then we use a redefined method of fundamental solutions (MFS) to determine the temperature and the normal heat flux on the inaccessible boundary. The present approach will give an ill-conditioned system, and this is a feature of the numerical method employed. In order to overcome the ill-posedness of the corresponding system, we use the Tikhonov regularization method combining Morozov's discrepancy principle to get a stable solution. At last, four numerical examples, including a smooth boundary, a boundary with a corner, and a boundary with a jump, are given to show the effectiveness of the present approach.

Keywords: Cauchy problem; Laplace equation; Half-plane; Single layer potential

1 Introduction

Cauchy problems, which arise in diverse science areas such as wave propagation, nondestructive testing, and geophysics have been intensively studied in the past decades [1, 7, 13, 33]. On account of the incomplete boundary conditions, Cauchy problems are classified as inverse problems and ill-posed, i.e., the solutions do not depend continuously on the Cauchy data. In order to get a stable solution, various numerical methods have been proposed to solve Cauchy problems [23, 31, 36]. The method of fundamental solutions (MFS) is a popular and frequently used method for the solution of such problems.

The MFS is a meshless method which expands the solution utilizing fundamental solutions [8, 16, 19, 20, 22, 28, 30, 39, 40]. It is a boundary collocation method which belongs to the family of Trefftz methods, see [14] for a link to Trefftz methods, boundary element methods, and MFS. It is applicable to boundary value problems in which the fundamental solution of the operator in the governing equation is known. Since then, it has been successfully applied to a large variety of physical problems, an account of which can be found in the survey paper [16]. In [26], Liu et al. introduce a novel concept to construct Trefftz energy bases based on the MFS for the numerical solution of the Cauchy problem in an arbitrary star plane domain. The Trefftz energy bases used for the solution not only satisfy the

Laplace equation but also preserve the energy. In [32], the authors give a meshless method based on the MFS for the three-dimensional inverse heat conduction problems. In [27], Marin investigates both theoretically and numerically the so-called invariance property of the solution of boundary value problems associated with the anisotropic heat conduction equation in two dimensions. In [9], Fu et al. investigate the thermal behavior inside skin tissue with the presence of a tumor and use the method of approximate particular solutions to simulate a tumor in 3D. Following Fichera's idea, Chen et al. [5] enriched the MFS by an added constant and a constraint. This enrichment condition ensures a unique solution of the problems considered. They also explained that this enrichment should be used when there is a degenerate scale. In [41], Zhang and Wei give two iterative methods for a Cauchy problem for an elliptic equation with variable coefficients in a strip region, the convergence rates of two algorithms are obtained by an a-priori and an a-posteriori selection rule for the regularization parameter. Other methods for the conduction problems can be found in [21, 37].

Cauchy problems have been investigated using the MFS because of the ease with which it can be implemented, particularly for the problems in complex geometries [10, 11, 25, 34]. Most of the studies consider Cauchy problems on the whole plane, but sometimes we should consider the problems in a half-plane [2, 3, 15, 24]. In [2], Chapko and Johansson consider a Cauchy problem for the Laplace equation in a two-dimensional semi-infinite domain by a direct integral equation method. Later, they give a generalization of the situation to three-dimensions with the Cauchy data only partially given. Compared with their previous work [2], they not only generalize that work to higher dimensions but also consider the more realistic case when the Cauchy data is only partially known, i.e., the Neumann/Dirichlet data measurements are specified throughout the plane bounding the upper half-space, and the Dirichlet/Neumann data is given only on a finite portion of this plane.

In this paper, we consider another Cauchy problem in a half-plane. Let D be a bounded and connected domain with piecewise smooth boundary $\partial D = \varGamma_1 \cup \varGamma_2 \cup \overline{AB}$, the upper boundary be $\varGamma = \varGamma_1 \cup \varGamma_2$. Define the half-plane $\mathbb{R}^2_+ := \{(x_1, x_2) : x_2 \geq 0\}$ and the boundary $\mathbb{R}^2_0 := \{(x_1, x_2) : x_2 = 0\}$. As is shown in Fig. 1, denote by

$$\varGamma := \bigl\{\boldsymbol{x} = \bigl(\rho(\theta)\cos\theta, \rho(\theta)\sin\theta\bigr), 0 \leq \theta \leq \pi\bigr\}$$

a simple piecewise smooth arc in $\mathbb{R}^2_+$ with two endpoints A and B on $\mathbb{R}^2_0$. The curve

$$\varGamma_1 := \{\boldsymbol{x} \in \varGamma, 0 \leq \theta \leq \beta\pi\}$$

is the accessible part of $\varGamma$ with $\beta \leq 1/2$.

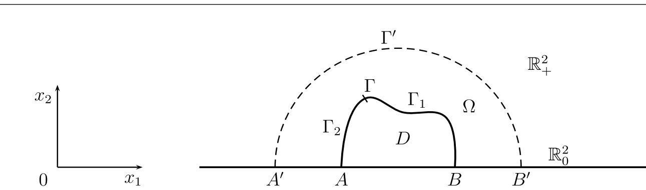

Figure 1 Sketch of the Cauchy problem in $\mathbb{R}^2_+$

Consider the following Cauchy problem for the Laplace equation: Given Cauchy data $f \in H^1(\varGamma_1)$ and $g \in L^2(\varGamma_1)$ on $\varGamma_1$ and the homogeneous boundary condition $u(\boldsymbol{x}) = 0$ on AB, find the solution u satisfying

$$\Delta u(\boldsymbol{x}) = 0, \quad \boldsymbol{x} \in D, \tag{1}$$

$$u(\boldsymbol{x}) = f(\boldsymbol{x}), \quad \boldsymbol{x} \in \varGamma_1, \tag{2}$$

$$\frac{\partial u}{\partial \nu}(\boldsymbol{x}) = g(\boldsymbol{x}), \quad \boldsymbol{x} \in \varGamma_1, \tag{3}$$

where Δ is the Laplacian in $\mathbb{R}^2$ and ν is the unit outward normal to $\varGamma_1$.

The Cauchy problem in a half-plane is novel since the solution of the problem should satisfy a Dirichlet boundary condition on part of the boundary AB and the Cauchy data on the accessible boundary $\varGamma_1$. We should note that a *Dirichlet boundary condition on part of the boundary is an essential condition* in the physical meaning. In this paper, for simplicity, we give a homogeneous boundary condition on the interface, i.e., the temperature is zero on the interface for a physical phenomenon.

In what follows, we describe a MFS for the numerical solution of the corresponding Cauchy problem. To prove the feasibility of the method, we use a single layer representation of the solution [18, 35]. Via the analysis of the single layer potentials, jump relations, and the Green's function in the half-plane, the solution given by the MFS is proved to be an approximation of the genuine solution. An "auxiliary" curve is involved in the definition of the single layer potential to avoid singularity.

This paper is organized as follows. In Sect. 2, we describe the MFS in a half-plane and give some theoretical results for this method. In Sect. 3, we solve the equations by the Tikhonov regularization method with Morozov's principle. Finally, four numerical examples, including a smooth boundary, a boundary with a corner, and a boundary with a jump, are presented to show the effectiveness of the presented method.

2 Formulation of the MFS

For $\boldsymbol{s} = (s_1, s_2) \in \mathbb{R}^2_+$, denote by $\boldsymbol{s}_r := (s_1, -s_2)$ the reflection of $\boldsymbol{s}$ about the x_1-axis. The Green's function of the Laplacian in the half space $\mathbb{R}^2_+$ with a Dirichlet boundary condition [29] is

$$G(\boldsymbol{x}, \boldsymbol{s}) = \frac{1}{2\pi} \ln |\boldsymbol{x} - \boldsymbol{s}| - \frac{1}{2\pi} \ln |\boldsymbol{x} - \boldsymbol{s}_r|, \tag{4}$$

where $\boldsymbol{s}$ is the source point and

$$|\boldsymbol{x} - \boldsymbol{s}| = \sqrt{(x_1 - s_1)^2 + (x_2 - s_2)^2}.$$

Note that the Green's function $G(\boldsymbol{x}, \boldsymbol{s})$ is the solution of

$$\Delta G(\boldsymbol{x}, \boldsymbol{s}) = \delta(\boldsymbol{x} - \boldsymbol{s}), \quad \boldsymbol{x} \in \mathbb{R}^2_+, \tag{5}$$

$$G(\boldsymbol{x}, \boldsymbol{s}) = 0, \quad \boldsymbol{x} \in \mathbb{R}^2_0, \tag{6}$$

where δ is the Dirac delta function.

To get the solution $u(\boldsymbol{x})$ of the Cauchy problem, we use the MFS approximation

$$u_N(\boldsymbol{x}) = \sum_{j=1}^{N} c_j G(\boldsymbol{x}, \boldsymbol{s}_j), \quad \boldsymbol{s}_j \in D_e, \tag{7}$$

where, for $j = 1, 2, \ldots, N$, $\boldsymbol{s}_j$ are the chosen source points in $D_e := \mathbb{R}^2_+ \setminus (\mathbb{R}^2_0 \cup \overline{D})$ and c_j are unknown coefficients, which can be computed using the Cauchy data on Γ_1.

For theoretical analysis, the single layer potential representation is involved, which can be seen as a continuous version of the MFS.

Denote by $\Gamma' := \partial\Omega \setminus \mathbb{R}^2_0$ the source curve (see Fig. 1), where $\partial\Omega$ is the boundary of the region $D \subset \Omega$ in $\mathbb{R}^2_+$. In fact, if the source points $\boldsymbol{s}_j$ are chosen on the curve Γ' with certain roles, approximation (7) can be viewed as a discrete version of the single layer potential in the half-plane

$$\left[S^h_{\Gamma'}\phi\right](\boldsymbol{x}) := \int_{\Gamma'} G(\boldsymbol{x}, \boldsymbol{y})\phi(\boldsymbol{y})\, \mathrm{d}s_{\boldsymbol{y}}, \quad \boldsymbol{x} \in \mathbb{R}^2_+ \setminus \Gamma'. \tag{8}$$

Notice that we involve an "auxiliary" curve Γ' in (8) instead of directly defining the single layer potential on ∂D. Then singularities caused by the integral equation in the single layer potential are avoided since Γ' is apart from $\overline{D}$. Another thing to notice is that the single layer potential (8) is related to the Green's function in the half-plane instead of that in the free space. Further analysis is needed to get the properties of the single layer potential.

Firstly, we recall the classical single layer potential in the free space. Assume that the endpoints of Γ' are $A' = (a', 0)$ and $B' = (b', 0)$ with $a' < b'$. Denote the unbounded region $\Omega^e := \{\mathbb{R}^2_+ \setminus \overline{\Omega}\}$ with the lower boundary $\Lambda := \Gamma'_- \cup \Gamma' \cup \Gamma'_+$, where $\Gamma'_- := \{\boldsymbol{x} = (x_1, 0) : x_1 \leq a'\}$ and $\Gamma'_+ := \{\boldsymbol{x} = (x_1, 0) : x_1 \geq b'\}$. Then the classical single layer potential on Λ is usually defined as

$$[S_\Lambda\phi](\boldsymbol{x}) := \int_\Lambda \Phi(\boldsymbol{x}, \boldsymbol{y})\phi(\boldsymbol{y})\, \mathrm{d}s_{\boldsymbol{y}}, \quad \boldsymbol{x} \in \mathbb{R}^2_+ \setminus \Lambda, \tag{9}$$

where $\Phi(\boldsymbol{x}, \boldsymbol{y})$ is the fundamental solution given by

$$\Phi(\boldsymbol{x}, \boldsymbol{y}) = \frac{1}{2\pi} \ln |\boldsymbol{x} - \boldsymbol{y}|.$$

Apparently we have

$$G(\boldsymbol{x}, \boldsymbol{y}) = \Phi(\boldsymbol{x}, \boldsymbol{y}) - \Phi(\boldsymbol{x}, \boldsymbol{y}_r). \tag{10}$$

Denote by ν the unit outward normal vector to Λ, where Ω^e is the exterior of the boundary Λ. For a curve Γ and a function u, denote by $\gamma^+_\Gamma u$ and $\gamma^-_\Gamma u$ the restrictions of u to Γ from exterior and interior, respectively. Denote by $\partial^+_{\nu,\Gamma} u$ and $\partial^-_{\nu,\Gamma} u$ the normal derivatives on Γ from exterior and interior, respectively.

We recall the jumps of a function on a curve. Denote by

$$[\![\gamma u]\!]_\Gamma = \gamma^-_\Gamma u - \gamma^+_\Gamma u$$

and

$$[\![\partial_\nu u]\!]_\Gamma = \partial^-_{\nu,\Gamma} u - \partial^+_{\nu,\Gamma} u$$

the jumps of u and $\partial_\nu u$ on Γ, respectively.

A symmetric continuation discussion shows that the Cauchy problem (1)–(3) is equivalent to the classical Cauchy problem with symmetric structure [3], which is well known to be uniquely solvable (for details, see [18]). Thus the Cauchy problem (1)–(3) also has a unique solution $u \in H^{3/2}(D)$.

Note that we only care about $u(\boldsymbol{x})$ for $\boldsymbol{x} \in \Omega$. Thus we can set

$$[\![\gamma u]\!]_{\Gamma'} = 0.$$

Then we have the following lemma about the single layer representation.

Lemma 1 *The solution of*

$$\begin{aligned}
&\Delta u(\boldsymbol{x}) = 0, \quad \boldsymbol{x} \in \mathbb{R}^2_+ \setminus \Gamma', \\
&[\![\gamma u]\!]_{\Gamma'} = 0, \quad \boldsymbol{x} \in \Gamma', \\
&u(\boldsymbol{x}) = 0, \quad \boldsymbol{x} \in \mathbb{R}^2_0
\end{aligned}$$

has the representation

$$u(\boldsymbol{x}) = \left[S^h_{\Gamma'}\phi\right](\boldsymbol{x}), \quad \boldsymbol{x} \in \mathbb{R}^2_+ \setminus \Gamma',$$

where the density function satisfies

$$\phi = [\![\partial_\nu u]\!]_{\Gamma'}.$$

Proof Since the single layer potential $[S^h_{\Gamma'}\phi](\boldsymbol{x})$ is formally an integral with the kernel $G(\boldsymbol{x},\boldsymbol{y})$, it is clear that $[S^h_{\Gamma'}\phi](\boldsymbol{x})$ satisfies the Laplace equation in $\mathbb{R}^2_+ \setminus \Gamma'$. Moreover, $G(\boldsymbol{x},\boldsymbol{y}) = 0$ for $y \in \mathbb{R}^2_0$ implies

$$u(\boldsymbol{x}) = 0, \quad \boldsymbol{x} \in \mathbb{R}^2_0.$$

The jump relation [15] implies that the density function satisfies

$$\phi = \left[\!\!\left[\partial_\nu \left(S^h_{\Gamma'}\phi\right)\right]\!\!\right]_{\Gamma'}.$$

The proof is completed. □

Although Lemma 1 gives the representation of the density function ϕ with the jump relation, ϕ is usually computed using boundary integral equations. Equations (2)–(3) imply that $S^h_{\Gamma'}\phi$ should satisfy

$$\left[S^h_{\Gamma'}\phi\right](\boldsymbol{x}) = f(\boldsymbol{x}), \quad \boldsymbol{x} \in \Gamma_1, \tag{11}$$

$$\frac{\partial[S^h_{\Gamma'}\phi]}{\partial\nu}(\boldsymbol{x}) = g(\boldsymbol{x}), \quad \boldsymbol{x} \in \Gamma_1. \tag{12}$$

We have the following proposition about the solution of the Cauchy problem.

Proposition 1 *Assume that $\phi \in L^2(\Gamma')$ is the solution of the boundary integral equations (11)–(12). Then the unique solution $u \in H^{3/2}(D)$ of the Cauchy problem (1)–(3) has the single layer representation*

$$u(\boldsymbol{x}) = \int_{\Gamma'} G(\boldsymbol{x},\boldsymbol{y})\phi(\boldsymbol{y})\,\mathrm{d}s_{\boldsymbol{y}}, \quad \boldsymbol{x} \in D. \tag{13}$$

Proof As we have discussed, $u = S^h_{\Gamma'}\phi$ satisfies the Laplace equation (1) and the Dirichlet boundary condition $u = 0$.

Since $\phi \in L^2(\Gamma')$ is the solution of the boundary integral equations (11)–(12), $u \in H^{3/2}(\Omega)$ satisfies the Cauchy boundary conditions (2)–(3) (for details of the spaces, see [18]). Thus $u|_D$ solves the Cauchy problem (1)–(3). The unique solvability of the Cauchy problem implies that the solution has representation (13).

This completes the proof. □

Finally, we give the following theorem for the MFS.

Theorem 1 *The MFS solution*

$$u_N(\boldsymbol{x}) = \sum_{j=1}^{N} c_j G(\boldsymbol{x},\boldsymbol{s}_j), \quad \boldsymbol{s}_j \in \Gamma' \tag{14}$$

is an approximation of the solution u to the Cauchy problem (1)–(3), where $\boldsymbol{s}_j$ are chosen as N equidistant discrete points on Γ' and

$$c_j = \frac{\mathrm{Len}(\Gamma')}{N}\phi(\boldsymbol{s}_j), \quad j = 1,2,\ldots,N,$$

in which $\mathrm{Len}(\Gamma')$ *is the length of Γ'.*

Proof Proposition 1 implies that the solution of the Cauchy problem (1)–(3) has representation (13). The discretization of the integral in (13) implies

$$u(\boldsymbol{x}) \approx \sum_{j=1}^{N} \frac{\mathrm{Len}(\Gamma')}{N} G(\boldsymbol{x},\boldsymbol{s}_j)\phi(\boldsymbol{s}_j),$$

where $\boldsymbol{s}_j$ are N equidistant discrete points on Γ' and $\mathrm{Len}(\Gamma')$ is the length of Γ'. Thus (14) is the approximation of the solution to (1)–(3). □

The coefficients c_j will be determined by a collocation method from the interpolation conditions at N_c collocation points. In fact, the coefficients c_j, $j = 1,2,\ldots,N$, are determined by solving a linear system of $2N_c$ equations, which consist of the boundary conditions at the N collocation points

$$Ac = b. \tag{15}$$

The matrix A, the unknown vector c, and the right-hand side b will be given by the following form:

$$A_{l,j} = G(\boldsymbol{x}_l, \boldsymbol{s}_j), \qquad A_{N_c+l,j} = \frac{\partial G(\boldsymbol{x}_{N_c+l}, \boldsymbol{s}_j)}{\partial \nu(\boldsymbol{x})},$$
$$b_l = f(\boldsymbol{x}_l), \qquad b_{N_c+l} = g(\boldsymbol{x}_l), \quad l = 1,\dots,N_c, j = 1,\dots,N.$$

In order to guarantee enough information to get a numerical solution, we need to choose N_c such that $N_c \geq \frac{N}{2}$.

3 Regularization method

In this section, we give a brief introduction to the Tikhonov regularization and Morozov's discrepancy principle, which are used to solve system (15). In general, the right-hand side vector b of system (15) consists of noise denoted by b^δ, so we should solve the following equation:

$$Ac^\delta = b^\delta. \tag{16}$$

The vector b^δ is the measured noisy data satisfying

$$b_i^\delta = b_i + \delta \operatorname{rand}(i) b_i,$$

where δ is the percentage noise and the number $\operatorname{rand}(i)$ is a pseudo-random number drawn from the standard uniform distribution on the interval $[-1, 1]$ generated by the Matlab command $-1 + 2\operatorname{rand}(i, 1)$.

The formally Tikhonov regularized solution of system (16) is given by

$$\bigl(\alpha I + A^\top A\bigr)c_\alpha^\delta = A^\top b^\delta. \tag{17}$$

From equation (17), we can see that the solution accuracy depends on the regularization parameter α, and hence how to choose an optimal regularization parameter α is crucial. There are some methods to choose a regularization parameter, such as the L-curve [12], the Cesàro mean in conjunction with the L-curve [6], Morozov's discrepancy principle [17], the multi-parameter Tikhonov regularization [38], the Gaussian window together with L-curve [4], etc. Especially when there is *a priori information* about the amount of noise available, we also use Morozov's discrepancy principle. We will choose the regularization parameter α by Morozov's discrepancy principle, which was developed in [33]. The computation of α can be carried out with Newton's method as follows:

1. Set $n = 0$, and give an initial regularization parameter $\alpha_0 > 0$;
2. Get $c_{\alpha_n}^\delta$ from $(A^*A + \alpha_n I)c_{\alpha_n}^\delta = A^* b^\delta$;
3. Get $\frac{\mathrm{d}}{\mathrm{d}\alpha} c_{\alpha_n}^\delta$ from $(\alpha_n I + A^*A)\frac{\mathrm{d}}{\mathrm{d}\alpha} c_{\alpha_n}^\delta = -c_{\alpha_n}^\delta$;
4. Get $F(\alpha_n)$ and $F'(\alpha_n)$ by

$$F(\alpha_n) = \bigl\|Ac_{\alpha_n}^\delta - b^\delta\bigr\|^2 - \delta^2$$

and

$$F'(\alpha_n) = 2\alpha_n \left\| A \frac{\mathrm{d}}{\mathrm{d}\alpha} c^{\delta}_{\alpha_n} \right\|^2 + 2\alpha_n^2 \left\| \frac{\mathrm{d}}{\mathrm{d}\alpha} c^{\delta}_{\alpha_n} \right\|^2,$$

respectively.

5. Set $\alpha_{n+1} = \alpha_n - \frac{F(\alpha_n)}{F'(\alpha_n)}$. If $\|\alpha_{n+1} - \alpha_n\| < \varepsilon$ ($\varepsilon \ll 1$), end. Else, set $n = n + 1$ and return to 2.

When the regularization parameter α^* is fixed, we can obtain the regularized solution.

4 Numerical experiments

In this section, we provide some numerical examples to show the effectiveness of the proposed method.

Example 1 The boundary is smooth, and the exact solution is chosen as

$$u(x_1, x_2) = e^{x_1} \sin x_2 + x_2^3 - 3x_2 x_1^2.$$

– Case 1: Γ is chosen as $\boldsymbol{x}_1 = (0.6 + 0.1 \cos 3t)(\cos t, \sin t)$, $t \in [0, \pi]$.
– Case 2: Γ is chosen as $\boldsymbol{x}_2 = (\cos t + 0.65 \cos 2t - 0.65, 1.5 \sin t)$, $t \in [0, \pi]$.
– Case 3: Γ is chosen as $\boldsymbol{x}_3 = 0.6\sqrt{4.25 + 2 \cos 3t}(\cos t, \sin t)$, $t \in [0, \pi]$.

First, we investigate the influence of the noise level on the numerical solution in case 1. The source curve Γ' is chosen as

$$\boldsymbol{x}_1' = 3(0.6 + 0.1 \cos 3t)(\cos t, \sin t), \quad t \in [0, \pi].$$

Choose $N = 50$, $N_c = 100$, and $\beta = 0.5$. The sketch can be seen in Fig. 2(a). Figure 2 shows the numerical solutions with different noise levels $\delta = 0.05$, $\delta = 0.1$, and $\delta = 0.15$, whilst it shows that our algorithm is effective and robust to random noise since the algorithm provides a smooth approximation of the solution.

Second, we consider the influence of β in case 2. Choose $N = 50$, $N_c = 100$, and $\delta = 0.05$. The source curve Γ' is chosen as

$$\boldsymbol{x}_2' = 2(\cos t + 0.65 \cos 2t - 0.65, 1.5 \sin t), \quad t \in [0, \pi].$$

The sketch can be seen in Fig. 3(a). Figure 3 shows the numerical solutions with $\beta = 0.3$, $\beta = 0.4$, and $\beta = 0.5$. From Fig. 3, it can be seen that the algorithm is effective with different choices of β and the error increases as β decreases, which is reasonable since the information of the Cauchy data is limited with small β.

To this end, the influence of the number N_c is investigated in case 3. Choose $N = 50$, $\beta = 0.5$, and $\delta = 0.05$. The source curve Γ' is chosen as

$$\boldsymbol{x}_3' = 1.2\sqrt{4.25 + 2 \cos 3t}(\cos t, \sin t), \quad t \in [0, \pi].$$

The sketch can be seen in Fig. 4(a). Figure 4(b) shows the relative errors with different choices of $N_c \in [25, 985]$. A decreasing trend of the error can be seen in Fig. 4(b) as N_c increases. The trend in the figure is unsharp since the noise added to the Cauchy data is

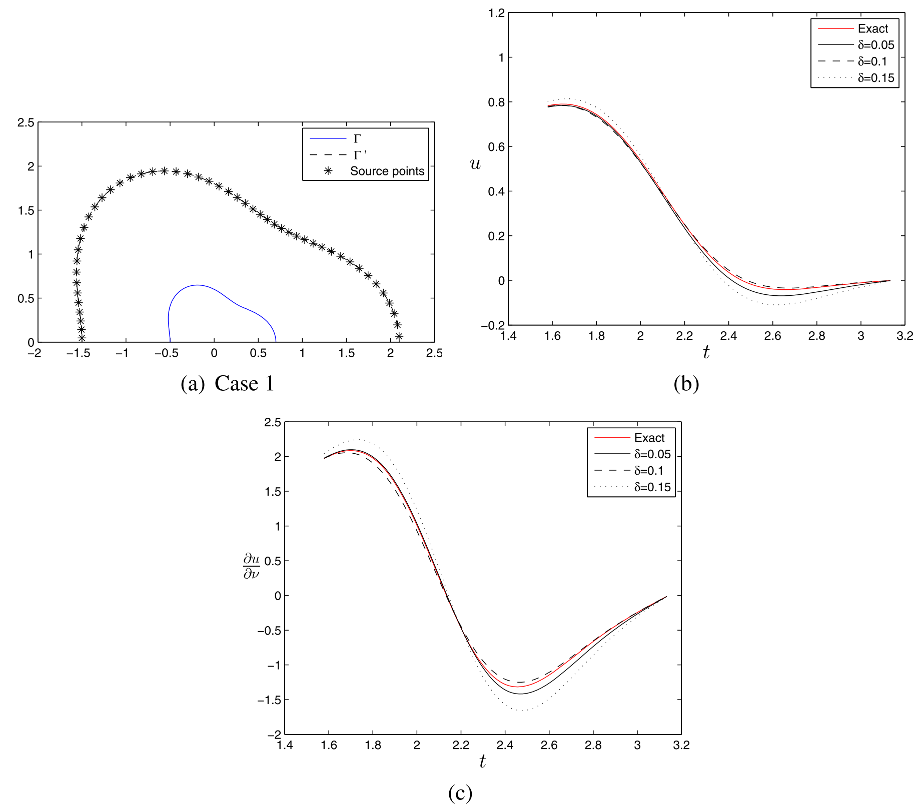

Figure 2 The exact solution and the numerical solutions on Γ_2 with $\delta \in \{0.05, 0.1, 0.15\}$

random, which means that the errors may change as we redo the experiment. Fortunately, the error changes within a limit and the decreasing trend of the errors can be observed from Fig. 4(b).

Example 2 In this example, Γ is continuous but with a "corner". The exact solution is chosen as

$$u_2(\boldsymbol{x}) = \mathrm{e}^{x_1} \sin x_2.$$

The curve Γ is chosen as the combination of

$$\boldsymbol{x}_4 = \frac{0.5}{\cos(0.25\pi - t)}(\cos t, \sin t), \quad t \in \left[0, \frac{\pi}{2}\right]$$

and

$$\boldsymbol{x}_5 = \frac{0.5}{\cos(0.75\pi - t)}(\cos t, \sin t), \quad t \in \left[\frac{\pi}{2}, \pi\right].$$

The source curve Γ' is chosen as

$$\boldsymbol{x}_4' = 1.5(\cos t, \sin t), \quad t \in [0, \pi].$$

Choose $N = 50$, $N_c = 100$, and $\beta = 0.5$. The sketch of Example 2 can be seen in Fig. 5(a).

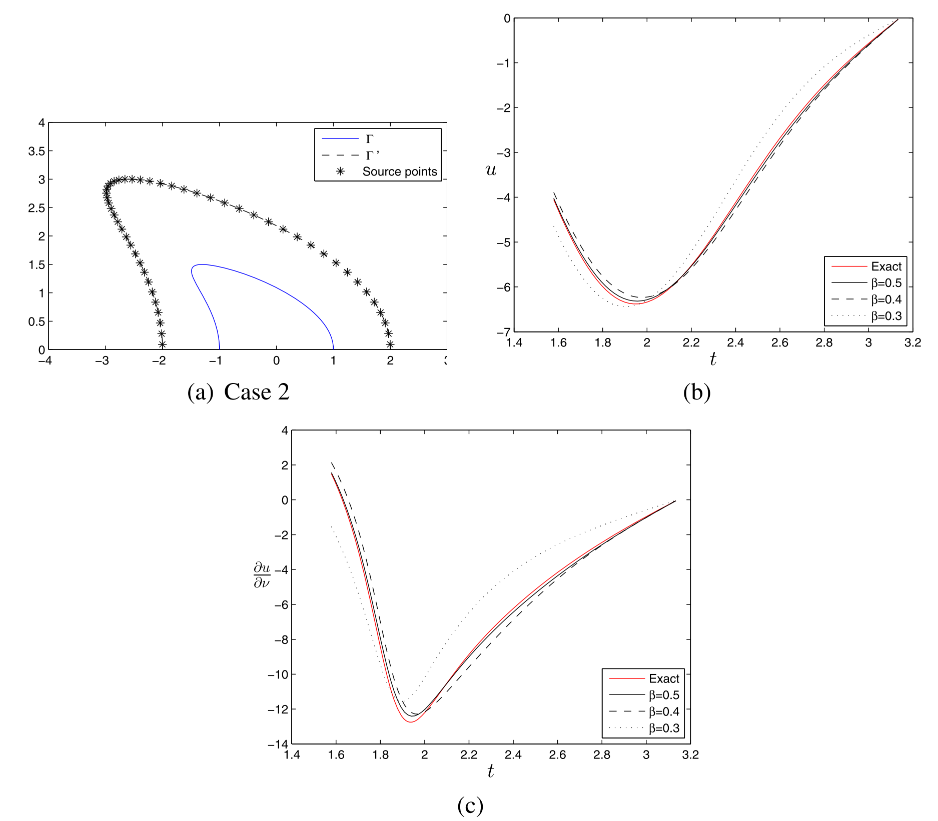

Figure 3 The exact solution and the numerical solutions on Γ_2 with $\beta \in \{0.3, 0.4, 0.5\}$

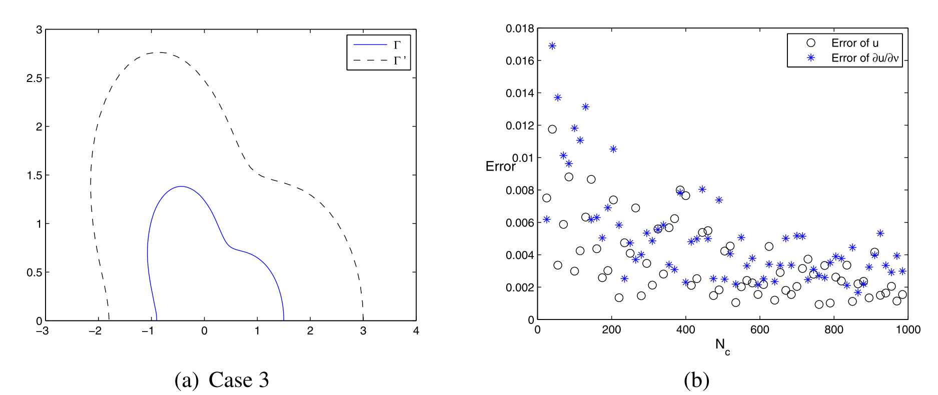

Figure 4 (**a**) Sketch of case 3. (**b**) The relative errors on Γ_2 with different choices of $N_c \in [25, 985]$

Figure 5 shows the numerical solutions with different noise levels $\delta = 0.01$, $\delta = 0.03$, and $\delta = 0.05$. As is shown in Fig. 5, the computation of $\frac{\partial u}{\partial \nu}$ is more sensitive to the error in this case.

Example 3 In this case, Γ has a jump at $t = \frac{\pi}{2}$. The exact solution is chosen as

$$u_3(\boldsymbol{x}) = \cosh x_1 \sin x_2.$$

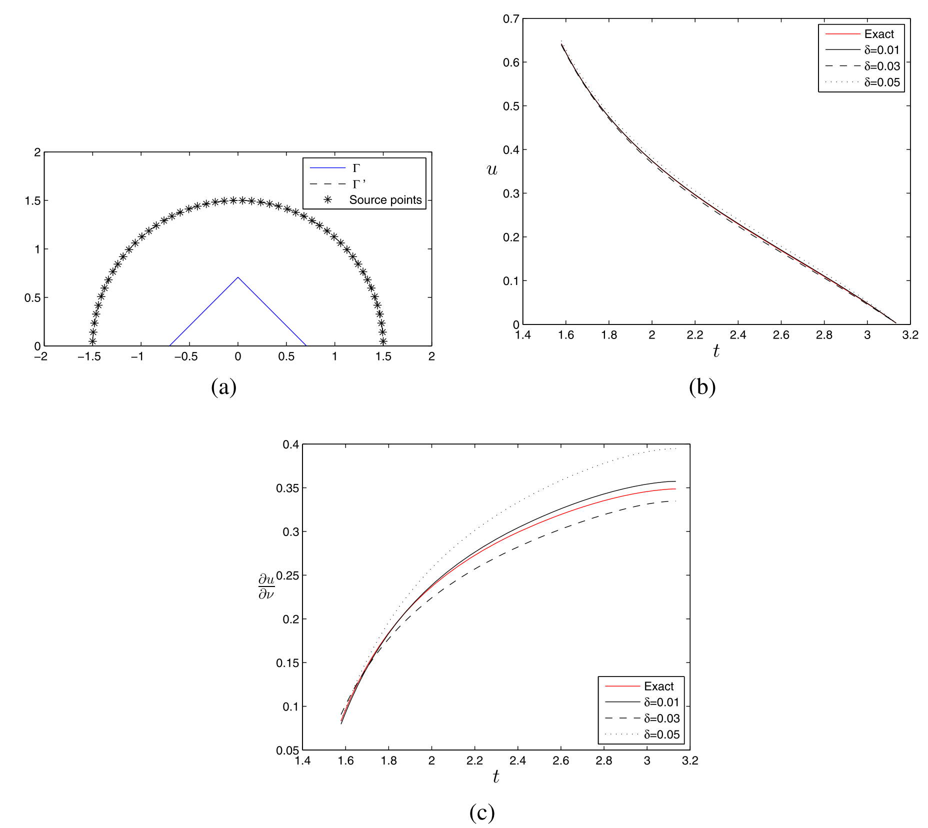

Figure 5 Example 2: The exact solution and the numerical solutions on Γ_2

The curve Γ is chosen as the combination of

$$\boldsymbol{x}_6 = \frac{0.5 + 0.4\cos t + 0.1\sin 2t}{1 + 0.7\cos t}(\cos t, \sin t), \quad t \in \left[0, \frac{\pi}{2}\right]$$

and

$$\boldsymbol{x}_7 = (0.6 + 0.1\cos 3t)(\cos t, \sin t), \quad t \in \left[\frac{\pi}{2}, \pi\right].$$

The source curve Γ' is chosen as $\boldsymbol{x}_4'$. Choose $N = 50$, $N_c = 100$, and $\beta = 0.5$. The sketch of Example 3 can be seen in Fig. 6(a). Figure 6 shows the numerical solutions with different noise levels $\delta = 0.01$, $\delta = 0.03$, and $\delta = 0.05$. It can be seen from Fig. 6 that the algorithm is still effective when Γ_1 is apart from Γ_2.

Example 4 In the previous examples, an analytic solution is available. We consider that the curve Γ is chosen by

$$\boldsymbol{x}_1 = (0.6 + 0.1\cos 3t)(\cos t, \sin t), \quad t \in [0, \pi].$$

Consider the following boundary value problem:

$$\Delta u(\boldsymbol{x}) = 0, \quad \boldsymbol{x} \in D, \tag{18}$$

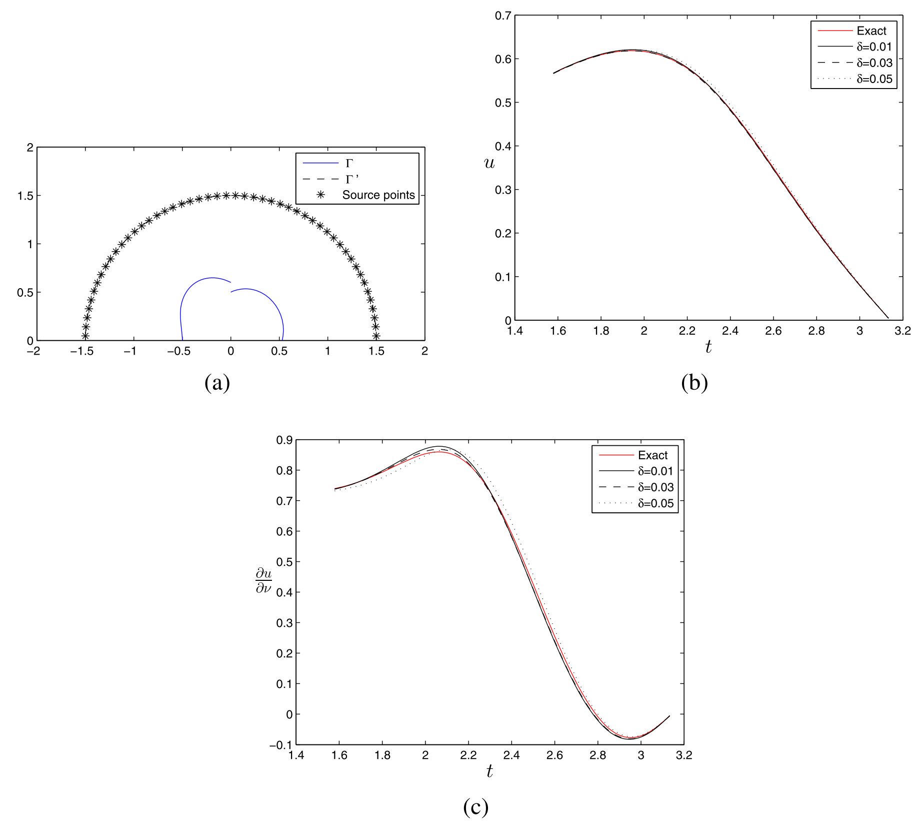

Figure 6 Example 3: The exact solution and the numerical solutions on Γ_2

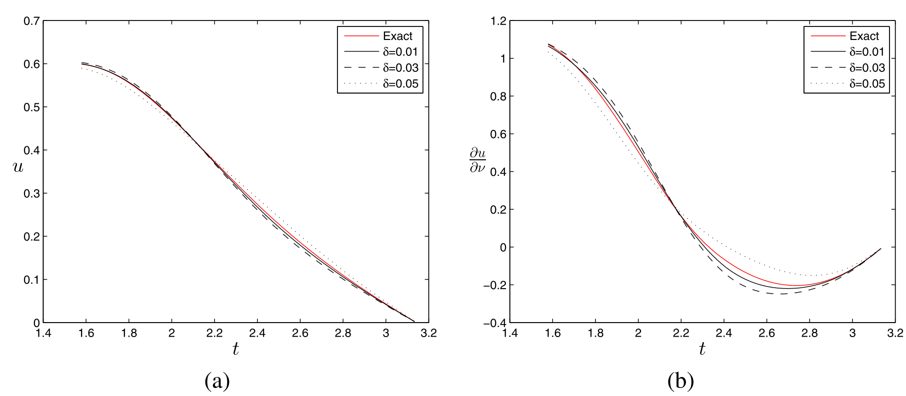

Figure 7 Example 4: The exact solution and the numerical solutions on Γ_2

$$u(\boldsymbol{x}) = x_2 e^{x_1}, \quad \boldsymbol{x} \in \partial D. \tag{19}$$

In this case, an analytic solution is not available. The input Cauchy data $f = x_2 e^{x_1}|_{\Gamma_1}$ and $g = \partial_n u|_{\Gamma_1}$, in which $g = \partial_n u|_{\Gamma_1}$ can be obtained numerically by solving the direct problem (18).

Figure 7 shows the numerical solutions for this case. It can be seen that the numerical solutions are stable approximations.

5 Conclusion

In this paper, we have dealt with a Cauchy problem connected with the Laplace equation in a half-plane. With the Green's function of the Laplacian in the half-plane, we have proposed a method of fundamental solutions to solve the Cauchy problem. Numerical experiments have also been given to show the effectiveness of the algorithm.

Acknowledgements
Not applicable.

Funding
This work is supported by the Youth Key Teacher Program of Civil Aviation University of China and the National Natural Science Foundation of China (Nos. U1433202, 11501566) and the Scientific Research Foundation of Civil Aviation University of China (No. 2017QD04S).

Availability of data and materials
Not applicable.

Competing interests
All the authors declare that they have no competing interests.

Authors' contributions
All of the authors contributed equally in writing this paper. All authors read and approved the final manuscript.

Author details
[1]College of Science, Civil Aviation University of China, Tianjin, China. [2]Flight Technology College, Civil Aviation University of China, Tianjin, China.

Publisher's Note

Received: 20 November 2018 Accepted: 5 February 2019 Published online: 12 February 2019

References

1. Bukhgeim, A.L., Cheng, J., Yamamoto, M.: Stability for an inverse boundary problem of determining a part of a boundary. Inverse Probl. **15**(4), 1021–1032 (1999)
2. Chapko, R., Johansson, B.T.: An alternating boundary integral based method for a Cauchy problem for the Laplace equation in semi-infinite domains. Inverse Probl. Imaging **2**, 317–333 (2008)
3. Chen, B., Ma, F., Guo, Y.: Time domain scattering and inverse scattering problems in a locally perturbed half-plane. Appl. Anal. **96**(8), 1–23 (2017)
4. Chen, J.T., Chen, K.H.: Analytical study and numerical experiments for Laplace equation with overspecified boundary conditions. Appl. Math. Model. **22**, 703–725 (1998)
5. Chen, J.T., Yang, J.L., Li, Y.T., Chang, Y.L.: Formulation of the MFS for the two-dimensional Laplace equation with an added constant and constraint. Eng. Anal. Bound. Elem. **46**, 96–107 (2014)
6. Chen, L.Y., Chen, J.T., Hong, H.K., Chen, C.H.: Application of Cesaro mean and the L-curve for the deconvolution problem. Soil Dyn. Earthq. Eng. **14**, 361–373 (1995)
7. Chen, W., Fu, Z.: Boundary particle method for inverse Cauchy problems of inhomogeneous Helmholtz equations. J. Mar. Sci. Technol. **17**(3), 157–163 (2009)
8. Fairweather, G., Karageorghis, A.: The method of fundamental solutions for elliptic boundary value problems. Adv. Comput. Math. **9**(1–2), 69–95 (1998)
9. Fu, Z.J., Xi, Q., Ling, L., Cao, C.Y.: Numerical investigation on the effect of tumor on the thermal behavior inside the skin tissue. Int. J. Heat Mass Transf. **108**, 1154–1163 (2017)
10. Gu, M.H., Young, D.L., Fan, C.M.: The method of fundamental solutions for one-dimensional wave equations. J. Mar. Sci. Technol. **11**(3), 185–208 (2009)
11. Gu, Y., He, X., Chen, W., Zhang, C.: Analysis of three-dimensional anisotropic heat conduction problems on thin domains using an advanced boundary element method. Comput. Math. Appl. **75**, 33–44 (2018)
12. Hansen, P.C.: Analysis of discrete ill-posed problems by means of the L-curve. SIAM Rev. **34**, 561–580 (1992)
13. Hon, Y.C., Wei, T.: Backus–Gilbert algorithm for the Cauchy problem of the Laplace equation. Inverse Probl. **17**(2), 261–271 (2001)
14. Hong, H.K., Chen, J.T.: Derivations of integral equations of elasticity. J. Eng. Mech. ASCE **114**, 1028–1044 (1998)
15. Hsiao, G.C., Wendland, W.L.: Boundary Integral Equations. Springer, Berlin (2008)
16. Karageorghis, A., Lesnic, D., Marin, L.: A survey of applications of the MFS to inverse problems. Inverse Probl. Sci. Eng. **19**(3), 309–336 (2011)
17. Kirsch, A.: An Introduction to the Mathematical Theory of Inverse Problems, 2nd edn. Springer, New York (2011)
18. Lee, J.Y., Yoon, J.R.: A numerical method for Cauchy problem using singular value decomposition. Commun. Korean Math. Soc. **16**(3), 487–508 (2001)
19. Li, J., Chen, W.: A modified singular boundary method for three-dimensional high frequency acoustic wave problems. Appl. Math. Model. **54**, 189–201 (2018)

20. Li, J., Chen, W., Fu, Z., Qin, Q.: A regularized approach evaluating the near-boundary and boundary solutions for three-dimensional Helmholtz equation with wideband wavenumbers. Appl. Math. Lett. **91**, 55–60 (2019)
21. Li, J., Chen, W., Gu, Y.: Error bounds of singular boundary method for potential problems. Numer. Methods Partial Differ. Equ. **33**, 1987–2004 (2017)
22. Li, J., Qin, Q.H., Fu, Z.: A dual-level method of fundamental solutions for three-dimensional exterior high frequency acoustic problems. Appl. Math. Model. **63**, 558–576 (2018)
23. Lin, J., Liu, C.S., Chen, W., Sun, L.: A novel Trefftz method for solving the multi-dimensional direct and Cauchy problems of Laplace equation in an arbitrary domain. J. Comput. Sci. **17**(3), 275–302 (2018)
24. Lin, J., Zhang, C., Sun, L., Lu, J.: Simulation of seismic wave scattering by embedded cavities in an elastic half-plane using the novel singular boundary method. Adv. Appl. Math. Mech. **10**(2), 322–342 (2018)
25. Liu, C.S.: A highly accurate MCTM for inverse Cauchy problems of Laplace equation in arbitrary plane domains. Comput. Model. Eng. Sci. **35**(2), 91–111 (2008)
26. Liu, C.S., Wang, F., Gu, Y.: Trefftz energy method for solving the Cauchy problem of the Laplace equation. Appl. Math. Lett. **79**, 187–195 (2018)
27. Marin, L.: An invariant method of fundamental solutions for two-dimensional steady-state anisotropic heat conduction problems. Int. J. Heat Mass Transf. **94**, 449–464 (2016)
28. Marin, L., Cipu, C.: Non-iterative regularized MFS solution of inverse boundary value problems in linear elasticity: a numerical study. Appl. Math. Comput. **293**, 265–286 (2017)
29. Polyanin, A.D.: Handbook of Linear Partial Differential Equations for Engineers and Scientists. Chapman & Hall/CRC, Boca Raton (2002)
30. Sun, Y.: Modified method of fundamental solutions for the Cauchy problem connected with the Laplace equation. Int. J. Comput. Math. **91**(10), 2185–2198 (2014)
31. Sun, Y.: Indirect boundary integral equation method for the Cauchy problem of the Laplace equation. J. Sci. Comput. **71**(2), 469–498 (2017)
32. Sun, Y., He, S.: A meshless method based on the method of fundamental solution for three-dimensional inverse heat conduction problems. Int. J. Heat Mass Transf. **108**, 945–960 (2017)
33. Sun, Y., Ma, F., Zhang, D.: An integral equations method combined minimum norm solution for 3D elastostatics Cauchy problem. Comput. Methods Appl. Mech. Eng. **271**, 231–252 (2014)
34. Sun, Y., Ma, F., Zhou, X.: An invariant method of fundamental solutions for the Cauchy problem in two-dimensional isotropic linear elasticity. J. Sci. Comput. **64**(1), 197–215 (2015)
35. Sun, Y., Zhang, D., Ma, F.: A potential function method for the Cauchy problem of elliptic operators. J. Math. Anal. Appl. **395**(1), 164–174 (2012)
36. Wang, F., Chen, W., Qu, W., Gu, Y.: A BEM formulation in conjunction with parametric equation approach for three-dimensional Cauchy problems of steady heat conduction. Eng. Anal. Bound. Elem. **63**, 1–14 (2016)
37. Wang, F.J., Chen, W., Gu, Y.: Boundary element analysis of inverse heat conduction problems in 2D thin-walled structures. Int. J. Heat Mass Transf. **91**, 1001–1009 (2015)
38. Wang, Z.: Multi-parameter Tikhonov regularization and model function approach to the damped Morozov principle for choosing regularization parameters. J. Comput. Appl. Math. **236**(7), 1815–1832 (2012)
39. Wei, T., Hon, Y.C., Ling, L.: Method of fundamental solutions with regularization techniques for Cauchy problems of elliptic operators. Eng. Anal. Bound. Elem. **31**, 373–385 (2007)
40. Wei, T., Zhou, D.: Convergence analysis for the Cauchy problem of Laplace's equation by a regularized method of fundamental solutions. Adv. Comput. Math. **33**, 491–510 (2010)
41. Zhang, H.W., Wei, T.: Two iterative methods for a Cauchy problem of the elliptic equation with variable coefficients in a strip region. Numer. Algorithms **65**(4), 875–892 (2014)